

Shear melting of a colloidal glass

Christoph Eisenmann, Chanjoong Kim,^{*} Johan Mattsson,[†] and David A. Weitz

*Department of Physics and HSEAS,
Harvard University, Cambridge, MA 02138, USA*

(Dated: February 4, 2009)

Abstract

We explore the microscopic nature of shear melting of colloidal glasses using confocal microscopy. We find that shear melting, which occurs at strains of $\sim 8\%$, coincides with a strongly non-Gaussian step size distribution, reflecting cooperative motions of ~ 3 particles. For large strains the particle mean square displacement increases linearly with strain and the step size distribution is Gaussian; the applied shear thus drives diffusive behavior. The effective diffusion coefficient varies approximately linearly with shear rate, consistent with a modified Stokes-Einstein relationship in which thermal energy is replaced by shear energy and the length-scale is set by the size of the cooperative regions.

PACS numbers: 61.43.Fs, 64.70.pv, 82.70.Dd

Colloidal suspensions provide a valuable model system for the study of the glass transition [1]. They exhibit many properties that mimic the behavior of more traditional molecular glass-formers; moreover, the large particle size and the slow dynamics, makes it possible to use direct imaging techniques to study the behavior of individual particles. This provides considerable new insight into features that are ubiquitous to the glass transition such as cooperativity and dynamic heterogeneity [2, 3]. However, colloidal glasses also possess features that are unique to them. Perhaps the most remarkable is shear melting. Because of the large particle size, colloids form soft solids; thus they can be fluidized through shear [4, 5], which can not be easily done for molecular glasses. Shear melting helps account for the widespread utility of these systems, since they can be solid-like under quiescent conditions, but can flow like a fluid when sheared. Such shear-induced fluidization is one means of driving a solid-to-fluid transition within the generic jamming 'phase'-diagram [6], wherein strong similarities should exist among shear-induced [7], concentration-induced and temperature-induced fluidization. However, a full understanding of the relationship of shear-induced fluidization to the other, more common methods of fluidization, requires a detailed understanding of the microscopic behavior of shear melting; this remains elusive.

In this Letter, we explore the microscopic nature of shear melting of colloidal glasses, by using confocal microscopy to measure the fluctuations of particle motion beyond the average imposed strain. We find that shear melting induces cooperative motion, extending over on average 3 particles, provided a characteristic strain of $\sim 8\%$ is exceeded. At large strains, the mean square displacement of the particles increases linearly with strain and the distribution of step sizes becomes Gaussian. Remarkably, this diffusive behavior can be accounted for by a modified Stokes-Einstein expression, where thermal energy is replaced by shear energy and the length-scale is set by the size of the cooperative regions.

We investigate a colloidal suspension of poly(methyl methacrylate) particles with an average diameter, $d = 1.2\mu\text{m}$ and a polydispersity of $\sim 4\%$. The particles are sterically stabilized with a thin layer of poly(hydroxy stearic acid), and are fluorescently labelled with nitrobenzoxadiazole. They are suspended in a mixture of cis-decalin and cycloheptylbromide, which matches both the particle density and index of refraction. To minimize the effects of charge on the particles, we add 1g/L of the salt tetrabutylammonium chloride [8]. The volume fraction is $\phi = 0.61 \pm 0.03$; this is a colloidal glass, as confirmed by its non-ergodic behavior probed by dynamic light scattering. The suspension is contained between two

parallel glass plates separated by a $40\mu\text{m}$ gap in a specially designed air-tight shear cell. The surfaces of the plates are roughened by a sintered coating of polydisperse particles (average radius = $1.5\mu\text{m}$ and polydispersity $\sim 30\%$) to avoid slip at the surface and to inhibit surface-induced ordering. We observed a linear shear gradient throughout the sample and did not detect any sign of crystallinity.

We follow the motions of individual colloidal particles under shear using confocal laser scanning microscopy; the particle positions are tracked as the suspension is subjected to a linear shear gradient. We focus the analysis on the central region of the suspension to avoid wall effects and restrict the analysis to a two-dimensional plane to allow us to follow the rapid motion of individual particles. A triangular saw-tooth time-dependent strain is applied to the sample in the y -direction with strain amplitudes reaching $\gamma \approx 0.5$ and strain periods varying between 25s and 100s, resulting in strain rates between 0.003s^{-1} and 0.02s^{-1} . The Péclet number, which determines the ratio of the shear rate to the rate of diffusion, is less than ≈ 0.1 if the self-diffusion coefficient of dilute particles, D_0 , is used. However, because we are investigating motion over length-scales that are comparable to the particle size the diffusion coefficient should more properly be chosen as the long-time diffusion coefficient, which reflects the structural relaxation of the particles and is many orders of magnitude larger than D_0 . As a result the effective Péclet number is very large and the motion is dominated by the imposed shear. To ensure reproducible results, the sample is subjected to strain for many periods at the chosen strain rate, after which data are collected for ten cycles at two frames per second. We track the position of each particle in the two dimensional plane and determine its position $x(t), y(t)$ after subtraction of the mean displacement due to the applied shear.

To investigate initiation of shear melting, we take advantage of the periodic application of strain and calculate an effective mean square displacement (MSD), $\langle \Delta x^2(\Delta t) \rangle_0 = \langle (x(t_0 + \Delta t) - x(t_0))^2 \rangle$, where t_0 is always taken as the initial time of a half-cycle and the averaging is repeated over 10 shear cycles. The behavior in the x and y directions are very similar, but the y component is about 30 – 50% larger, consistent with previous results [9, 10] and presumably reflecting the anisotropy expected as a result of Taylor dispersion [11], Since the qualitative behavior is so similar, here we focus only on the x component, $\langle \Delta x^2(\Delta t) \rangle_0$.

Since the motion is driven by the strain, we plot the MSD as a function of the strain

accumulated during the lag time, Δt , allowing us to compare the data obtained at all strain rates. In all cases the behavior of the MSD is nearly identical: For strains below $\gamma \approx 0.08$, subdiffusive behavior is observed; this is followed by a crossover to a diffusive regime, as shown in Fig. 1 (a). This behavior is reminiscent of that found for materials that shear melt at a critical strain [5]. To explore whether our results are consistent with such behavior, we calculate the MSD averaged over start times, t_y , chosen after the onset of diffusive behavior, corresponding to a strain above $\gamma \approx 0.08$, $\langle \Delta x^2(\Delta t) \rangle_y = \langle (x(t_y + \Delta t) - x(t_y))^2 \rangle$. As shown in Fig. 1 (b), we find a similar behavior for every start time implying that the observed behavior does not reflect a critical strain. This result is consistent with previous findings of both 'in-cage' rattling motions [10] and a significant elastic contribution [5] for shear melted colloidal hard sphere glasses at strains well above 7 – 15%.

The distribution of particle displacements in the liquid state of a colloidal suspension is Gaussian. By contrast, as the glass transition is approached, strongly non-Gaussian behavior is observed reflecting the existence of dynamic heterogeneities [12]. To examine the behavior of a shear melted glass, we determine the displacement distribution function $P(\Delta x(\Delta t))$. For large lag times, corresponding to strains greater than ~ 0.08 , the distribution is Gaussian, consistent with liquid-like dynamics; by contrast, for short lag-times corresponding to $\gamma < 0.08$, the distribution is strongly non-Gaussian and is instead better described as exponential, as shown in the inset to Fig. 1 (a). This suggests that the motion is highly heterogeneous at small strains, but becomes much more homogeneous at large strains.

We can further quantify the observed behavior by calculating the non-Gaussian parameter $\alpha_2(t) = \frac{\langle \Delta x^4 \rangle}{3\langle \Delta x^2 \rangle^2} - 1$, which is zero for Gaussian dynamics and non-zero otherwise. To compare the data, we normalize α_2 for each data set by its maximum. Independent of the starting time, we find identical behavior for the normalized α_2 ; it reaches a maximum at a strain of ~ 0.08 independent of the strain rate, as shown in Figs. 1 (c) and (d). This maximum corresponds to the crossover of the MSD between subdiffusive and diffusive behavior. Similar behavior is observed for a colloidal liquid near its glass-transition [3], where α_2 reaches a maximum at the onset of structural relaxation and particle flow.

To explore the nature of the non-Gaussian behavior, we calculate the two-point correlation function $D_{rr}(r, \Delta t) = \langle \Delta r^i(\Delta t) \Delta r^j(\Delta t) \rangle_{|r^i - r^j| = r}$, where $\Delta r^i(\Delta t)$ is the projection of the displacement onto the vector between the two particles [13]. For any continuum material either fluid or solid $D_{rr}(r, \Delta t) \sim 1/r$; a deviation from this behavior is direct evidence

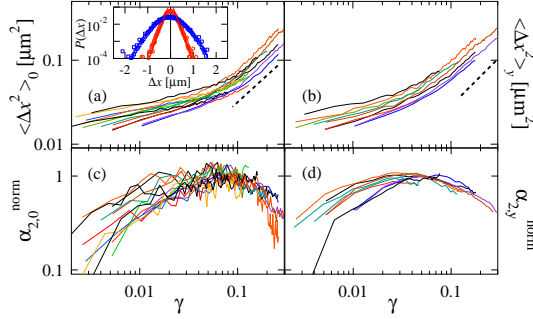


FIG. 1: (a) $\langle \Delta x^2(\Delta t) \rangle_0$ versus strain γ of a sheared colloidal glass for different strain rates varying from 0.003s^{-1} to 0.02s^{-1} . Inset: Distribution function $P(\Delta x(\Delta t))$ for the sheared glass ($\dot{\gamma} = 0.02\text{s}^{-1}$) for $\Delta t = 4\text{s}$ (red squares) and $\Delta t = 50\text{s}$ (blue circles) together with an exponential and a Gaussian fit, respectively. (b) $\langle \Delta x^2(\Delta t) \rangle_y$ vs strain, calculated with a start time always chosen in the 'yielded' regime. (c) Non-Gaussian parameter α_2 calculated from the data in (a) as a function of strain. α_2 has been normalized by its maximum value. (d) Normalized α_2 calculated from the data in (b).

of anomalous particle dynamics. We therefore calculate rD_{rr} , to sensitively explore the range of the $1/r$ behavior. For long delay times the data follow a straight line with zero slope, as shown in Fig. 2 (a). However, as the delay time decreases, the data instead exhibit an increasingly sharp decay. These results suggest the onset of a new shear-induced behavior. To quantify this behavior we calculate the ratio of rD_{rr} measured at $r = 10\mu\text{m}$ and $r = 3\mu\text{m}$; a value of 1 corresponds to $D_{rr} \approx 1/r$, whereas a smaller value indicates faster decay. We plot this ratio as a function of strain and find an exponential growth from zero to a value near 1, as shown in Fig. 2 (b). An exponential fit gives a characteristic strain of ≈ 0.08 , in accord with the strain amplitude where the MSD crosses over from subdiffusive to diffusive behavior; moreover, this crossover is consistent with the change in the step-size distribution at the same strain amplitude. These data suggest that small strains result in highly heterogeneous particle motion, whereas at large strains the heterogeneous motions have spread fully through the sample leading to effectively homogeneous motion. These small-strain motions are clearly reminiscent of dynamic heterogeneities observed on approach to the glass-transition [3, 14].

To further explore the nature of cooperative motions in the sheared sample, we quantify the range of cooperativity in the particle motions. We focus on particles that move further

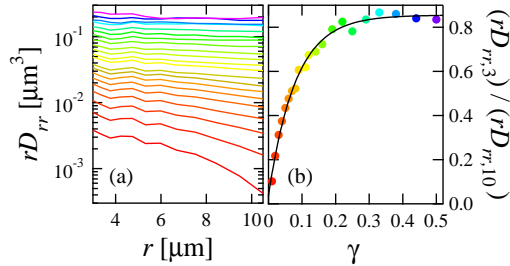


FIG. 2: (a) Two-point correlation function D_{rr} , multiplied by r for a sheared glass ($\dot{\gamma} = 0.02\text{s}^{-1}$) for different lag times ranging from $\Delta t = 0.5\text{s}$ (red) to $\Delta t = 25\text{s}$ (purple). (b) Ratio of rD_{rr} at $r = 10\mu\text{m}$ and $r = 3\mu\text{m}$ versus accumulated strain. The line is an exponential fit with a characteristic strain $\gamma_c = 0.08$.

than a threshold distance, δ , within a lag-time, Δt , corresponding to a fixed accumulated strain in the diffusive regime. We find that the particular choice of strain and threshold distance is not critical and any reasonable choice of parameters characterizing the diffusive regime gives very similar results; typically, we use a threshold distance $\delta \simeq 0.3\mu\text{m} \simeq d/4$ and a strain $\gamma \simeq 0.15$. We color-code the particles with respect to their direction of movement: Particles with a large displacement component in the positive x-direction, $\Delta\vec{r}(\Delta t) \cdot \hat{x}/\Delta r \geq 0.8$ and $\Delta r(\Delta t) \geq \delta$, are colored in green; analogously orange is used for motions in the -x while red and blue are used for the +y and -y directions, respectively. We compare the cooperative particle motions of a shear melted glass to those of a low ϕ ($\sim 40\%$) volume fraction colloidal liquid with a comparable diffusion coefficient. Snapshots of the particle motions as shown in Fig. 3 document the development of larger clusters for the shear melted glass than for the unsheared low volume fraction liquid. Interestingly, we observe clusters of particles moving both parallel and perpendicular to the direction of the applied strain.

To quantitatively compare the average dynamic cluster size for the low volume fraction liquid and the sheared glass, we plot the dynamic cluster size distribution for each sample. Two particles of the same color were assigned to the same dynamic cluster if the interparticle distance was less than the first minimum in the distinct radial distribution function. We find that the sheared glass has a longer tail of large dynamic clusters, as shown in Fig. 3. Integrating the data, we obtain an average dynamic cluster size of about 2-3 particles, setting the scale of the cooperative motion of the dynamic heterogeneities. We do not find any shear-rate dependence of this size within the accuracy of the measurements. This size

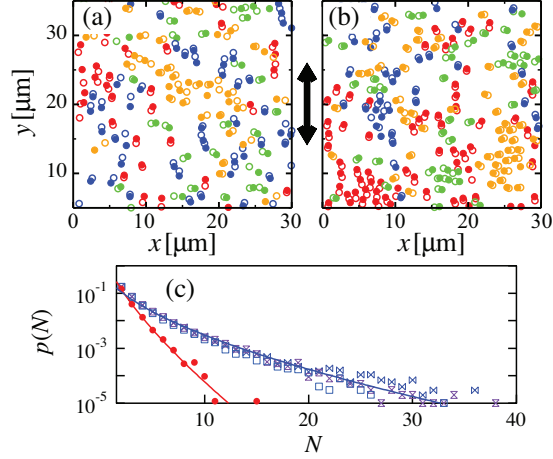


FIG. 3: Dynamic clusters for a low volume fraction, $\sim 40\%$, liquid (a) and a sheared glass with $\dot{\gamma} = 0.01\text{s}^{-1}$ (b). The full symbols indicate particle positions at $t = t_0$, the open symbols positions at $t = t_0 + 15\text{s}$, corresponding to an accumulated strain of $\gamma = 0.15$. Red/blue: moving in $\pm y$ -direction. Green/orange: moving in $\pm x$ -direction. The sample is sheared in the y -direction. For clarity, particle sizes are not drawn to scale. (c) Size-histogram for the dynamic clusters of the shear-melted glass (blue empty symbols) for various shear rates from 0.008 to 0.021s^{-1} , at the same accumulated strain of $\gamma = 0.15$ and the unsheared low-volume fraction liquid (red filled circles). The lines are guides to the eye.

is in good agreement with the measurements of shear transformation zones observed in a colloidal glass subjected to small strains and low strain rates [14].

A further comparison between the fluid sample and the shear melted sample is obtained by measuring the shear induced diffusion coefficient for the particle motion. We calculate the MSDs for the shear-melted sample as $\langle \Delta x^2(t) \rangle_y$ and find that the MSDs are linear in time as shown in Fig. 4 (a). From linear fits to the data, we extract the long-time diffusion constants of the shear melted glass from $\langle \Delta x^2(t) \rangle_y = 2Dt$. The increase of the diffusion constant, D , with strain rate, $\dot{\gamma}$, is consistent with a linear behavior, as shown in Fig. 4 (b). A similar behavior was observed in a simulation that approximated the behavior of a 2D foam at zero temperature [15]; in fact, these data are in good agreement with ours when we scale the characteristic foam size to the size of our colloidal particles, see Fig. 4 (b). This surprising similarity in the observations suggests that the behavior might be quite general for shear melted glassy samples. We note, however, that a recent study of a shear-melted

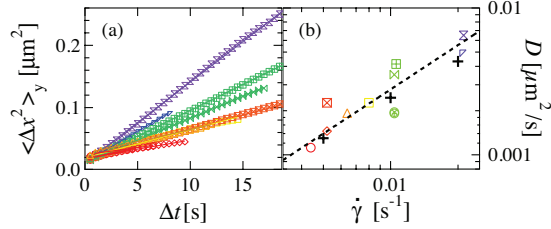


FIG. 4: (a) $\langle \Delta x^2(\Delta t) \rangle_y$ as a function of lag time, Δt , for a shear-melted glass at different applied strain rates. The lines are linear fits to the data. (b) Long-time diffusion coefficient, D , extracted from the linear fits in (a), as a function of strain rate $\dot{\gamma}$. The symbols correspond to those of the data in (a) except the + symbols, showing data taken from ref. [15]. The dashed line corresponds to $D = \frac{2}{9}R_s^2\dot{\gamma}$, with $R_s = 0.9d$; d is the particle diameter.

hard-sphere colloidal glass suggested a slightly sublinear scaling, $D \propto \dot{\gamma}^{0.8}$ [10].

To account for an approximately linear dependence of the diffusion constant with strain rate, we consider an analogy to the Stokes-Einstein expression for an equilibrium fluid, $D = k_B T / 6\pi\eta R$, which is the ratio of the thermal energy to the friction factor. To describe the behavior of the diffusion constant of the shear melted samples, we replace the thermal energy term by the shear energy, given by the product of the viscosity and the strain rate $\frac{4\pi}{3}R_s^3\eta\dot{\gamma}$, where R_s is the radius of a characteristic volume. The friction factor is then $6\pi\eta R_s$ and the diffusion coefficient is $D = \frac{2}{9}R_s^2\dot{\gamma}$. This expression is consistent with the approximately linear dependence of $\dot{\gamma}$ observed in the data. Moreover, we obtain quantitative agreement between this expression and the data by using $R_s = 0.9d$, as shown by the dashed line in Fig. 4 (b). The characteristic radius, R_s , corresponds to a volume containing about 3-4 particles, in excellent accord with the direct measurements of the average size of the dynamic clusters. If the scaling were sublinear, R_s would decrease slightly for increasing shear rates.

Our results suggest that a shear-melted glass exhibits many similarities to a colloidal suspension that has been fluidized by reduction of its volume fraction or a glass that has been fluidized by increase of its temperature. We observe the signatures of dynamic heterogeneities, but only at small strains; at larger strains, these are averaged out and the particle motion becomes effectively homogeneous. We find that particles move cooperatively involving on average 3 particles. Remarkably, we can describe the diffusion behavior observed at large strains in the shear-melted glass with a modified Stokes-Einstein expression. This

intriguing result supports the possibility that shear can be regarded as an 'effective temperature' [15]. However, whether a highly driven non-equilibrium system can be described with concepts from equilibrium statistical mechanics needs further investigation.

We thank D. R. Reichman, F. C. MacKintosh and A. J. Liu for helpful discussions. This work was supported by the NSF (DMR-0602684), the Harvard MRSEC (DMR-0213805), the Deutsche Forschungsgemeinschaft (CE), and by the Hans Werthén, the Wennergren and the Knut and Alice Wallenberg Foundations (JM).

* Present address: Chemical Physics Interdisciplinary Program, Liquid Crystal Institute, Kent State University, Kent, OH 44242, USA.

† Present address: Dept. of Applied Physics, Chalmers University of Technology, SE-412 96, Göteborg, Sweden.

- [1] W. van Meegen and S. M. Underwood, *Phys. Rev. Lett.* **70**, 2766 (1993).
- [2] W. K. Kegel and A. van Blaaderen, *Science* **287**, 290 (2000).
- [3] E. R. Weeks, J. C. Crocker, A. C. Levitt, A. Schofield, and D. A. Weitz, *Science* **287**, 627 (2000); E. R. Weeks and D. A. Weitz, *Phys. Rev. Lett.* **89**, 095704 (2002).
- [4] T. G. Mason and D. A. Weitz, *Phys. Rev. Lett.* **75**, 2770 (1995).
- [5] G. Petekidis, A. Moussad and P. N. Pusey, *Phys. Rev. E* **66**, 13 (2002); G. Petekidis, D. Vlassopoulos and P. N. Pusey, *Faraday Discuss.* **123**, 287 (2002); K. N. Pham, G. Petekidis, D. Vlassopoulos, S. U. Egelhaaf, P. N. Pusey, and W. C. K. Poon, *Europhys. Lett.* **75**, 624 (2006).
- [6] A. J. Liu and S. R. Nagel, *Nature* **396**, 21 (1998).
- [7] M. Fuchs and M. E. Cates, *Phys. Rev. Lett.* **89**, 248304 (2002); K. Miyazaki and D. R. Reichman, *Phys. Rev. E* **66**, 050501 (2002); K. Miyazaki, H. M. Wyss, D. A. Weitz, and D. R. Reichman, *Europhys. Lett.* **75**, 915 (2006); H. M. Wyss, K. Miyazaki, J. Mattsson, Z. Hu, D. R. Reichman, and D. A. Weitz, *Phys. Rev. Lett.* **98**, 238303 (2007).
- [8] A. Yethiraj and A. van Blaaderen, *Nature (London)* **421**, 513 (2003).
- [9] D. J. Pine, J. P. Gollub, J. F. Brady, and A. M. Leshansky, *Nature* **438**, 997 (2005)
- [10] R. Besseling, E. R. Weeks, A. B. Schofield, and W. C. K. Poon, *Phys. Rev. Lett.* **99**, 028301 (2007).

- [11] G. I. Taylor, Proc. R. Soc. London A **219**, 186 (1954); **223**, 446 (1954).
- [12] P. Chaudhuri, L. Berthier, and W. Kob, Phys. Rev. Lett. **99**, 060604 (2007).
- [13] J. C. Crocker, M. T. Valentine, E. R. Weeks, T. Gisler, P. D. Kaplan, A. G. Yodh, and D. A. Weitz, Phys. Rev. Lett. **85**, 888 (2000).
- [14] P. Schall, D. A. Weitz, and F. Spaepen, Science **318**, 1895 (2007).
- [15] I. K. Ono, C. S. O'Hern, D. J. Durian, S. A. Langer, A. J. Liu, and S. R. Nagel, Phys. Rev. Lett. **89**, 095703 (2002).